Separation Science and Technology
Publication details, including instructions for authors and subscription information:
http://www.informaworld.com/smpp/title~content=t713708471

Transient Behavior of Lithium Isotope Separation by Displacement Chromatography

S. Fujine[a]; K. Saito[a]; K. Shiba[a]
[a] DIVISION OF NUCLEAR FUEL RESEARCH JAPAN ATOMIC ENERGY RESEARCH INSTITUTE TOKAI, IBARAKI, JAPAN

To cite this Article Fujine, S. , Saito, K. and Shiba, K.(1982) 'Transient Behavior of Lithium Isotope Separation by Displacement Chromatography', Separation Science and Technology, 17: 11, 1309 — 1325
To link to this Article: DOI: 10.1080/01496398208056104
URL: http://dx.doi.org/10.1080/01496398208056104

SEPARATION SCIENCE AND TECHNOLOGY, 17(11), pp. 1309–1325, 1982

Transient Behavior of Lithium Isotope Separation by Displacement Chromatography

S. FUJINE, K. SAITO, and K. SHIBA

DIVISION OF NUCLEAR FUEL RESEARCH
JAPAN ATOMIC ENERGY RESEARCH INSTITUTE
TOKAI, IBARAKI, JAPAN

Abstract

Lithium isotope concentration profiles at the steady and unsteady states are obtained using the circuit for continuous displacement chromatography, which is composed of 2 cm i.d. columns packed with the strong-acid cation exchange resin, Diaion SK116 (100 μm). These profiles agree well with the results calculated assuming lithium adsorption bands to be square cascades in total reflux operation.

INTRODUCTION

Lithium isotope separation using ion exchangers has been studied by many researchers since Taylor and Urey made experiments on synthetic zeolite in 1937 (*1*). Glueckauf first applied synthetic, organic ion exchangers to separating lithium isotopes (*2*); the use of a breakthrough technique and lithium acetate gave a sharp front boundary. Powell also made similar experiments (*3*).

Lee systematically measured the single-stage separation factors for lithium isotopes by varying the parameters: the temperature, the nature and concentration of eluents, the exchange functional groups, and the degree of cross-linkage of resins (*4–8*). The separation factors were found to be 1.0003–1.0047.

The isotope effects were multiplied by various separation processes. Blanco and Roberts separated lithium isotopes using a continuous countercurrent contactor in which ion-exchange resins moved upward and a solution of sodium acetate was fed into the top of the lithium band. The reflux

operation was carried out at both ends of the band (*9*). Hagiwara separated the isotopes by displacement chromatography in the fixed beds of ion-exchange resins by using calcium acetate and barium acetate as displacement reagents (*10–12*). However, the isotope concentration profiles were not sufficiently studied.

We consider that displacement chromatography in fixed beds is superior to the continuous countercurrent contactor because the amount of liquid mixing in the lithium band is much smaller for the former than for the latter. Lithium isotope separation factors are infinitely small in a single stage, so that the loss of separation effect by liquid mixing should be minimized. We set up equipment for continuous displacement chromatography composed of several fixed beds of ion-exchange resins, and carried out experiments on lithium isotope separation in order to study the transient behavior.

We have indicated in a report (*13*) that the profiles could be calculated using theories for square cascades in a total reflux operation. The isotope concentration profiles of the unsteady states were calculated for a natural lithium feed. In the present work, lithium isotope concentration profiles of the steady and unsteady states are obtained experimentally with equipment for continuous displacement chromatography, and are studied on the basis of the theory of displacement chromatography.

Principle of Lithium Isotope Separation by Displacement Chromatography

Lithium isotope separation is promoted by dehydration of lithium ions when they are adsorbed by resins, as explained by Lee et al. (*4*). Since water molality is reduced in the resin phase and the water structure is disrupted by the presence of the organic matrix, lithium ions are less strongly hydrated and hence less strongly bonded in the resin phase than in the dilute solution surrounding the resin particles. The heavier isotope, ^{7}Li, which tends to concentrate preferentially in the more strongly bonded species (*14*), thus favors the aqueous phase, and ^{6}Li is exchanged into the resin. The magnitude of the separation factor is determined primarily by the degree of hydration of the lithium species in the aqueous and resin phases.

Figure 1 shows the procedure of lithium isotope separation by displacement chromatography. A lithium adsorption band is formed on the H-form resin bed, and sodium acetate as a displacement reagent is introduced into the top of the band. Lithium ions are desorbed at the rear boundary and displace hydrogen ions at the front boundary. While the band moves in columns with fixed length, lithium isotopes are exchanged between the resin and solution phases. Lithium isotope concentration profiles are formed in the

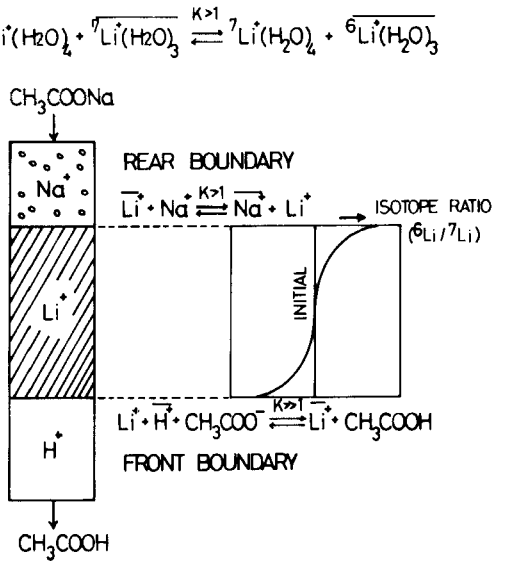

FIG. 1. Principle of lithium isotope separation by displacement chromatography. (The horizontal bars represent the resin phase.)

band. Acetates are used in order to sharpen the front boundary as explained by Powell (*3*).

Although the selectivity coefficient $K = 2.57$ between Na^+ and Li^+ is relatively small, we chose Na^+ ions as the displacement agent because the Na-form resins are easily regenerated with a smaller amount of HCl than the Ca^{2+} and Ba^{2+} form resins which were used by Hagiwara (*11*).

EXPERIMENTAL

Equipment

Figure 2 shows the flow sheet of the experimental equipment; a circuit for continuous displacement chromatography and the accompanying apparatus (*15*). The circuit is composed of 10 columns; every column has two 2 cm i.d. $\times$ 1 m Pyrex tubes, each attached to a water jacket and a movable plug.

The columns are packed with the strong acid cation exchange resin Diaion SK116, a gel type with sulfonic acid groups, a mean diameter of 100 μm, a

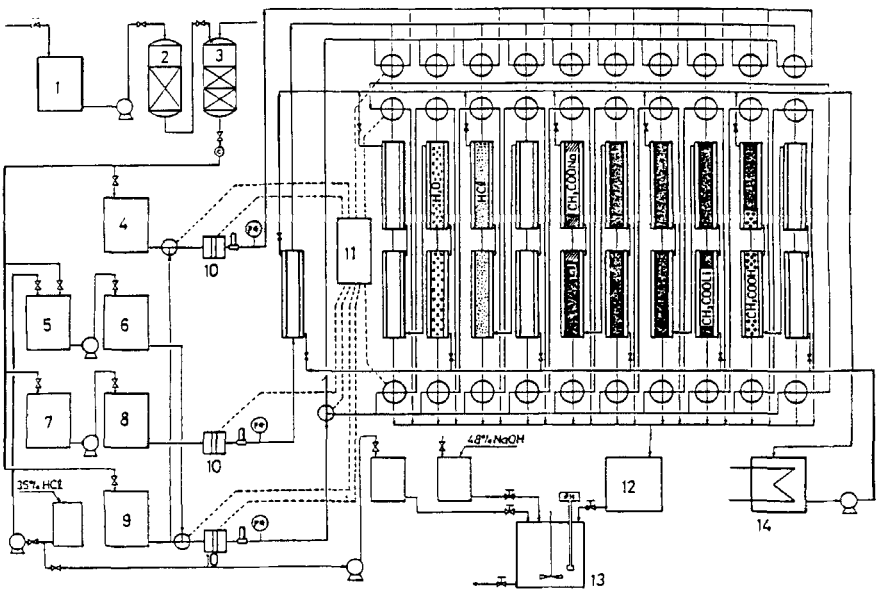

FIG. 2. Experimental equipment for continuous displacement chromatography. 1: Water. 2: Active carbon. 3: Ion exchange resin. 4: Lithium solution. 5: Preparation of HCl. 6: 2*N* HCl storage. 7: Preparation of displacement reagent. 8: Storage of displacement reagent. 9: Pure water. 10: Planger pump. 11: Control system. 12: Storage of waste. 13: Neutralization of waste. 14: Temperature control unit.

degree of cross-linkage of 16% DVB, and an ion-exchange capacity of $q_0 =$ 2.66 meq/mL.

The valves between the columns are automatically operated by signals from a control system, and the reagents can be fed into the columns in turn according to fixed time schedules. The operations of displacement of lithium adsorption band, regeneration of the resins, and back-washing and rinsing by pure water are repeated periodically. Planger pumps feed the chemical reagents at constant flow rates into the circuit. Teflon tubes of 1 mm i.d. connect these columns, valves, and pumps. The circuit withstands up to 30 kg/cm^{2}G, where G is gauge pressure. The temperature is set at 20°C.

Experimental Conditions

Experiments were carried out using natural lithium of 92.58% ^{7}Li isotope concentration. Sodium acetate of 0.5 mol/L concentration is fed into the circuit as the displacement reagent at a flow rate of 1.0 m/h superficial

velocity for most cases. Lithium adsorption bands move at a speed of 17.8 cm/h in this case.

The isotope concentration in the samples was analyzed by the optical spectrometric method using a hollow cathode lamp as the luminous source, calibrated by mass spectrometry (*17*). The concentrations of Li and Na were analyzed by flame photometry.

RESULTS

Isotope Separation Factors

Lithium isotope separation factors depend on the physicochemical characteristics of a system such as structure of resin matrix, functional groups, ionic strength of external solution, temperature, and coexisting ions in both phases. Therefore, the factors were obtained for the present system using the breakthrough technique. The technique gives accurate separation factors as expressed by Spedding et al. (*16*). Applying their method to the present system of lithium isotope separation, one obtains the separation factor α by

$$\alpha = 1 + \sum_{i=1}^{m} \frac{v_i C_i | R_0 - R_i |}{QR_0} \tag{1}$$

where v_i (mL) is the volume of the effluents collected fractionally, C_i (mol/L) is the concentration of lithium in the effluents, R_i is the isotope ratio (^{6}Li/^{7}Li), $R_0 = 0.082$ of natural isotope ratio of lithium fed into the column, and Q (meq) is the total capacity of ion-exchange resin in the columns. The equation is based on the definition of the separation factor as follows:

$$\alpha = \frac{\overline{N}}{1 - \overline{N}} \Big/ \frac{N}{1 - N} \tag{2}$$

where $\overline{N}$ and N are the isotope mol fractions in the resin and liquid phases, respectively. The value 1.0028 for the separation factor was obtained from the experiment. The identical separation factor was also observed for different superficial velocities. The value is almost equal to those obtained by Blanco (*9*), Lee (*7*), Powell (*3*), and Hagiwara (*10*), but is far smaller than 1.0071 for Diaion SK116 described in the latest report of Hagiwara (*12*).

Concentration Profiles in Bands

Figure 3 shows the profiles of lithium isotope, Li, Na, and H in the effluents obtained by the displacement of a 7-m long band for 1080 h. This corresponds to the displaced distance 190 m. The species ^7Li is enriched at the front boundary of the band; the species ^6Li is enriched at the rear boundary. The initial, natural concentration of 92.58% ^7Li remains over 3 m length in the middle part of the band, which forms a plateau in the isotope concentration profile. If the displacement had been continued, the plateau would have become shorter, and it would disappear from the profile at the steady state. The midway isotope concentrations at 430 h and the displaced distance 77 m are also plotted in the figure. The figure shows that the gradient of the concentration profile near the boundaries of the band become less steep with time.

Since the valence of H^+, Li^+, and Na^+ ions is identical, the concentrations of lithium acetate and acetic acid in the effluent are equal to the concentration of sodium acetate $C_0 = 0.5$ mol/L. Band length l_B (cm) is related to the effluent volume V (mL) by

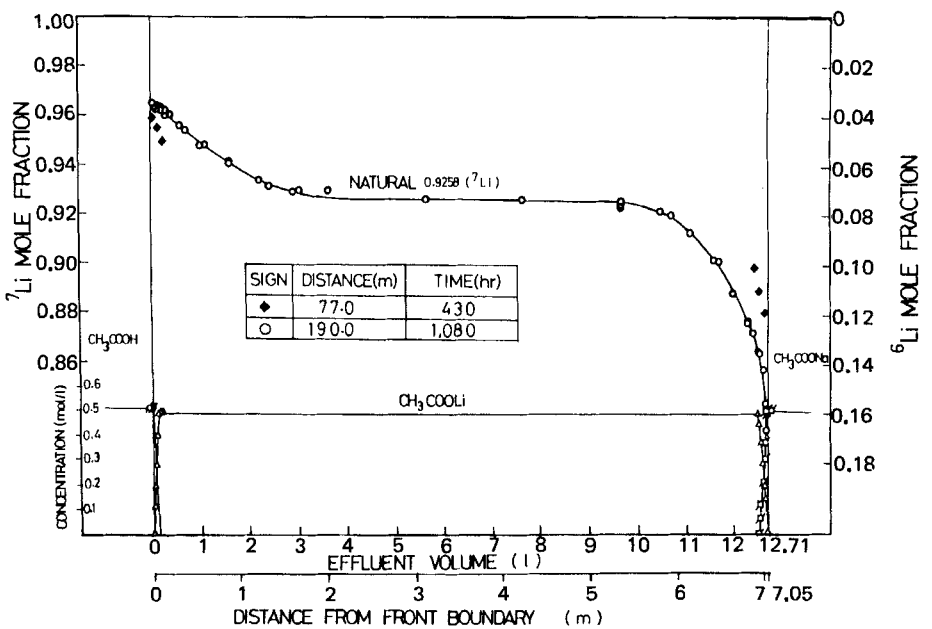

FIG. 3. Profiles of lithium isotope, Li, Na, and H obtained by displacement of a 7-m long band.

$$l_B = C_0 V/\{\pi r^2(q_0 + \varepsilon C_0)\} \quad (3)$$
$$= 0.056V$$

where ε is the void fraction of the resin beds and has a value of 0.35. The symbol r is the radius of the columns. From calculation by Eq. (3), lithium and the neiboring ions are found to overlap at 5.6 cm at the front end of lithium band and at 11.2 cm at the rear end. This difference of lengths reflects the difference of selectivity coefficients at the front and rear ends of the band.

Figure 4 shows the operation conditions of the run. Since the flow rate of sodium acetate is set to be constant, the displaced distance of the band becomes longer in proportion with time. The band moves at a constant speed of 17.8 cm/h with the length fixed. The feed pressure of sodium acetate is 7–9 kg/cm^{2}G. The height of the resin bed fluctuates periodically as the lithium band passes through the column. The magnitude of the fluctuation becomes smaller with time, and at last settles at about 1% of the total height of the resin bed. The height of the resin bed in the tube measures 93.5 cm on average.

In the case of displacement of shorter bands, steady states are attained more quickly. Figure 5 shows the profiles obtained by the displacement of a 56.3-cm long band. Since the superficial velocity of the displacement reagent is set to be 0.5 m/h in this run, the band moves at 9.0 cm/h. The isotope concentration profiles do not change from 470 h on. This indicates that the

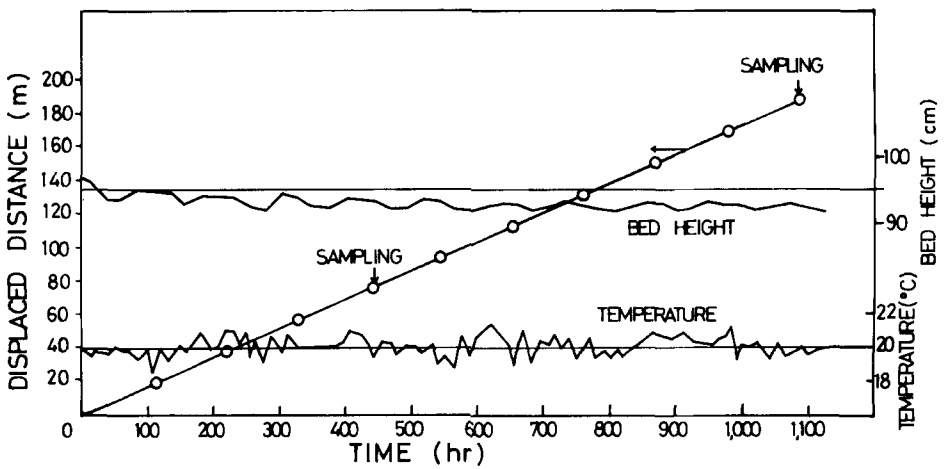

FIG. 4. Operation conditions.

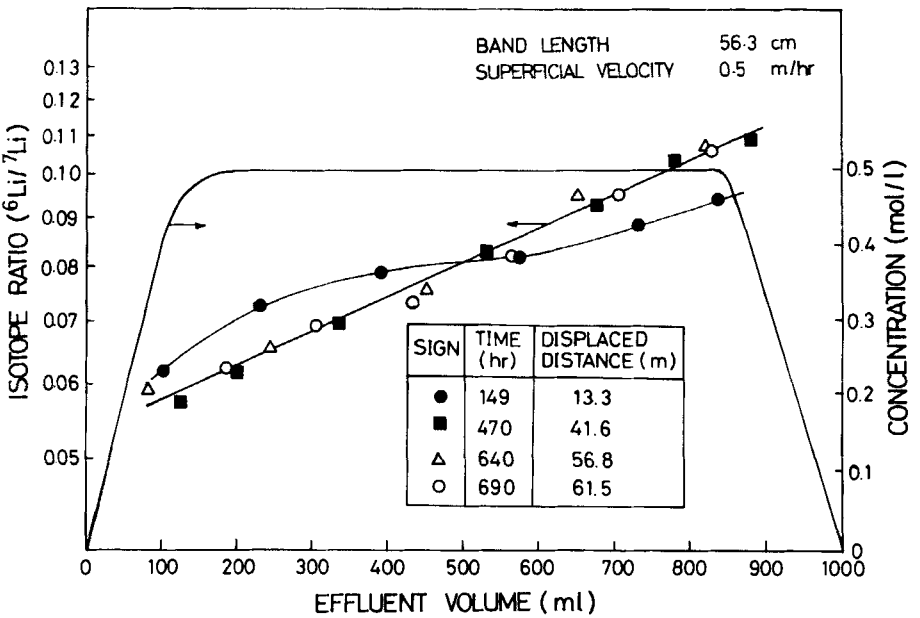

FIG. 5. Profiles of lithium isotope and Li obtained by displacement of a 56.3-cm long band.

steady state has already been attained by that time; the displaced distance is 41.6 m.

Figure 6A shows the Li isotope concentration profiles at several times as obtained by the displacement of a 91.1-cm long band. The superficial velocity of displacement reagent is set at 1.0 m/h in this run. Steady state has been attained by 722 h; the displaced distance is 128.5 m. The profile at the steady state is found to be linear on the semilogarithmic ordinates. This indicates that the following Fenske's equation holds:

$$S = \ln \frac{R'}{R''} \Big/ \ln \alpha \tag{4}$$

where R' and R'' are the isotope ratios. The symbol S is the number of theoretical stages, which is also related to the band length and the height equivalent to a theoretical plate (HETP) $\triangle z$ (cm) by

$$S = l_B / \triangle z \tag{5}$$

Equation (4) is known to give the concentration profiles for square cascades in a total reflux operation.

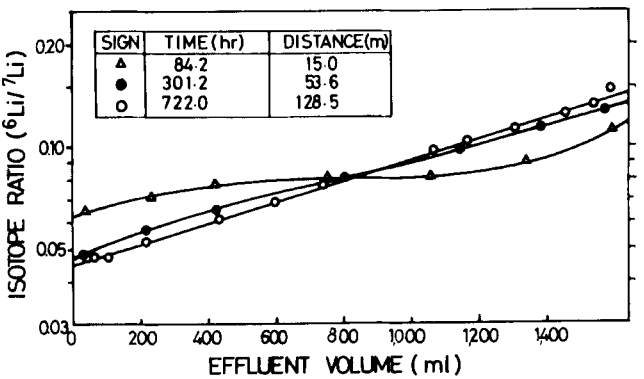

FIG. 6A. Lithium isotope concentration profiles obtained by displacement of a 91.1-cm long band.

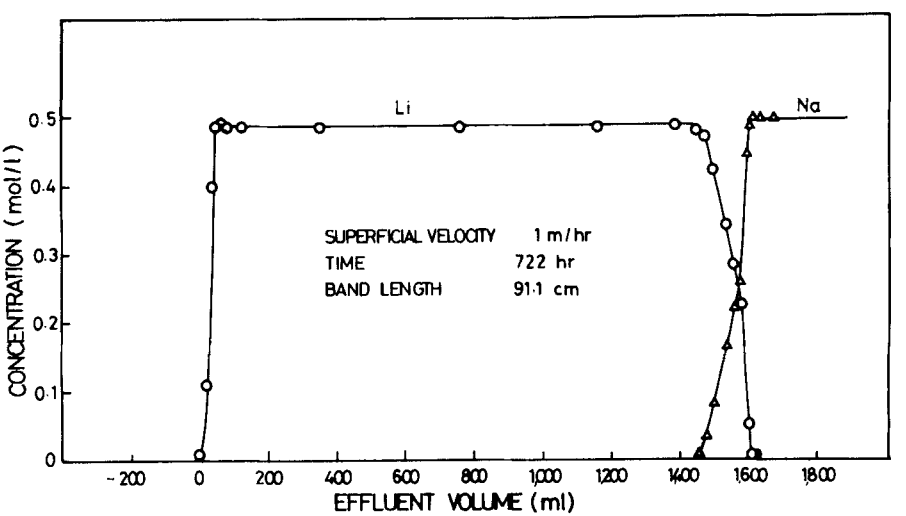

FIG. 6B. Profiles of Li and Na.

Figure 6B shows the concentration profiles of Li and Na in the effluents for the run of Fig. 6A. The overlapping lengths of lithium ions with the neighboring ions are measured to be 3 and 9 cm for the front and rear ends of the band, respectively. These lengths are shorter than those for the run of 7-m long band. The difference is affected by the difference in the liquid volumes above the resin beds in the columns. The heights are measured to be about 5.8 cm for the 7-m long band, and shortened to about 3.6 cm by using the movable plugs for the 91.1-cm long band. The liquid mixing in the liquid volumes above the resin beds seriously reduces the spearation potential in the circuit of displacement chromatography. The shorter heights of the volumes resulted in shorter overlapping lengths of the neighboring ions.

DISCUSSION

Observation indicates that Li adsorption bands move in the columns while keeping constant band length and maintaining both boundaries fairly sharp. For these conditions a band can be assumed to be a countercurrent contactor with total reflux occurring at the boundaries. If the bands are looked from the coordinate system as moving at the same speed as the bands, the following equation is derived as described in Ref. *13*:

$$\frac{\partial N}{\partial \tau} = \frac{\partial^2 N}{\partial s^2} - (\alpha - 1)\frac{\partial}{\partial s}\{N(1 - N)\} \tag{6}$$

where τ is the dimensionless time expressed by

$$\tau = \frac{L'}{H_0}t = \frac{q_0}{(q_0 + \varepsilon c_0)}\frac{u_B}{\triangle z}t \tag{7}$$

where L' (mol/s) is the theoretical interstage flow rate, H_0 (mol) is the lithium holdup in a theoretical stage, and u_B (cm/s) is the speed of the moving band. Equation (6) gives the isotope concentration profiles in bands at an arbitrary time. For the steady state, Eq. (6) becomes the Fenske's Eq. (4) by using $\alpha - 1 \approx \ln \alpha$. The linear relation between the stage number S and $\ln R$ is verified by the present experiment. Since the isotope separation factor is assumed to be constant throughout the band, the total number of theoretical stages is obtained by applying Eqs. (3) and (4) to the concentration profile at the steady state. The HETP is obtained from Eq. (5).

The isotope concentration profiles at unsteady states can be calculated using Eq. (6) with an appropriate HETP, because the necessary physico-

chemical factors, except HETP, can be measured. However, the equation is too difficult to solve for general cases, and the general, transient profiles are numerically calculated by assuming the lithium band as an imaginary square cascade as shown in Fig. 7. The band is composed of many theoretical stages. The bottom stage is adjacent to the front boundary and the top stage to the rear boundary. Both boundaries are assumed to be the plates vertical to the flow in the column.

The concentration changes are expressed using the dimensionless time τ for the top stage ($s = S$)

$$dN_S/d\tau = \overline{N}_{S-1} - N_S \tag{8}$$

for the arbitrary stages ($s \neq 1, S$)

$$dN_s/d\tau = \overline{N}_{s-1} + N_{s+1} - \overline{N}_s - N_s \tag{9}$$

for the bottom stage ($s = 1$)

$$dN_1/d\tau = N_2 - \overline{N}_1 \tag{10}$$

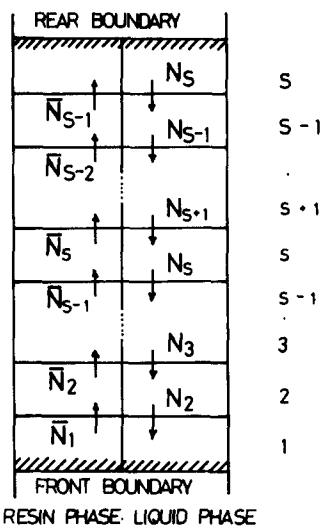

FIG. 7. Imaginary square cascade.

Equation (2) is changed into

$$\overline{N}(s) = A(s)N(s) \tag{11}$$

where

$$A(s) = \frac{\alpha}{1 + (\alpha - 1)N(s)} \tag{12}$$

Since the isotope concentration change per stage is very small, the functions of $N(s)$ and $A(s)$ can be approximated by the differentials of Taylor's expansion. The terms of the first and second differentials are used for $N(s)$ except for the ends ($s = 1, S$). Since the differential $\partial A(s)/\partial s$ is very small, the relation of $A(s) \approx A(s + 1)$ is assumed, and the following basic equations are obtained:

$$\frac{\partial N}{\partial \tau} = (1 - A)N - \frac{\partial N}{\partial s} \qquad (s = S) \tag{13}$$

$$\frac{\partial N}{\partial \tau} = \frac{1}{2}(A + 1)\frac{\partial^2 N}{\partial s^2} + (A - 1)\frac{\partial N}{\partial s} \qquad (s \neq 1, S) \tag{14}$$

$$\frac{\partial N}{\partial \tau} = (A - 1)N + A\frac{\partial N}{\partial s} \qquad (s = 1) \tag{15}$$

The constancy of total holdup H_T (mol) in the band, furthermore, gives the following condition:

$$dH_T/d\tau = 0 \tag{16}$$

These equations are solved numerically in the same way described in Ref. *13*. Namely, the representative stages are chosen at regular intervals in the imaginary square cascade; the partical differentials of Eqs. (13), (14), and (15) are approximated by the finite differences using the concentrations of the representative stages; and the linear differential equation system obtained is solved using the Runge-Kutta-Merson method.

The isotope concentration profiles were calculated for the conditions of the present experiment by using a value of 1.0028 for the separation factor. Figure 8 illustrates the profiles calculated for several total stage numbers with the experimental data of displacement of the 7-m long band shown in

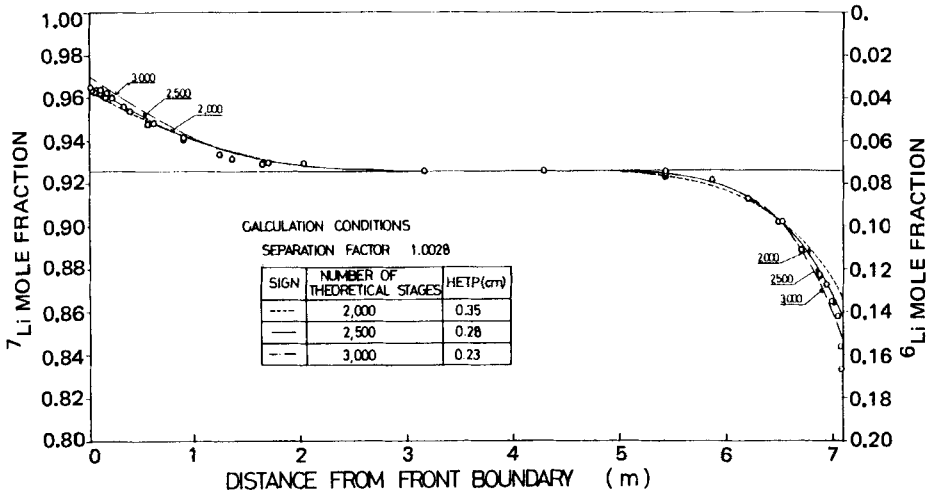

FIG. 8. Lithium isotope concentration profiles calculated for several total stage numbers and experimental data for the 7-m long band.

Fig. 3. The best agreement exists in the case with a total stage number of 2500. This corresponds to a HETP of 2.8 mm.

Figures 9A, 9B, and 9C illustrate the fitting of profiles obtained by the displacement of the 91.1-cm long band. In this case the isotope concentration profiles for the unsteady and steady states are obtained under the same experimental conditions. The single value of HETP, however, does not give the best agreement for all the profiles. The profile at 84.2 h agrees best for a total stage number of 900 and a HETP 1 mm, as shown in Fig. 9A. The profile at 301 h agrees best for a HETP of 1.8 mm, as shown in Fig. 9B. And HETP becomes 2.1 mm at 722 h when the steady state has been attained.

The HETP obtained increases with time to a fixed value of the steady state as shown in Fig. 10. The similar behavior of HETP increasing is explicitly revealed in Fig. 3 which shows the isotope concentration profiles obtained by the displacement of the 7-m long band. The gradient of the concentration profile near the boundaries of a band becomes less steep with time. This means that HETP increases with time. The phenomenon may be due to liquid mixing in the columns. Figure 4 shows that the height of the resin beds reduces to a settled value while fluctuating periodically; that is, the liquid volume above the bed increases to a constant amount during the process of displacement. The liquid volume which exists in each tube of the circuit affects the concentration profiles, especially for the displacement chromatography of bands. The HETP, found to be 2.8 and 2.1 mm at the steady state

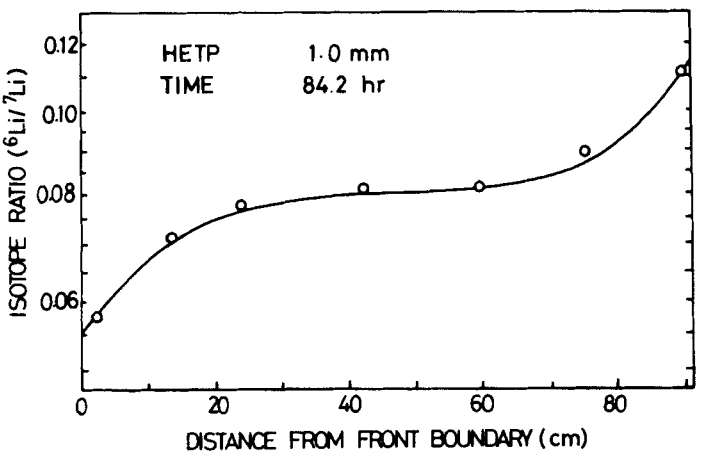

FIG. 9A. The fitting of profiles for the displacement of a 91.1-cm long band.

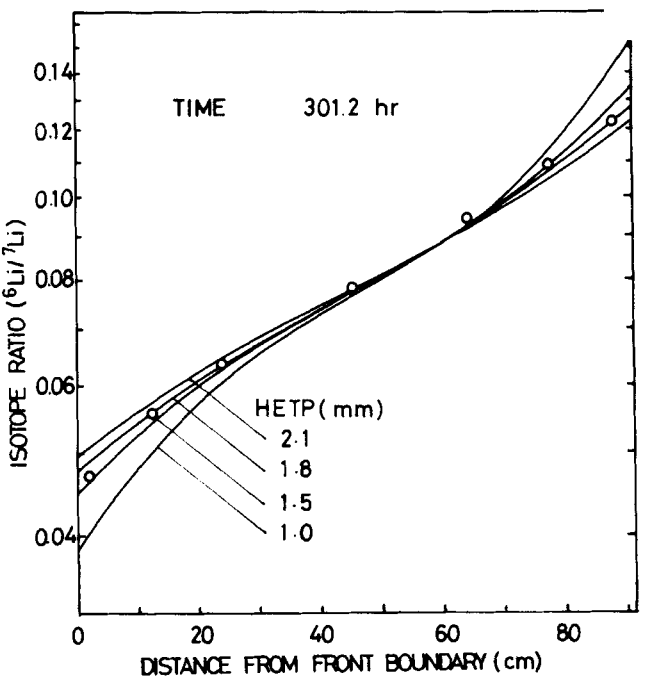

FIG. 9B. The fitting of profiles for the displacement of a 91.1-cm long band.

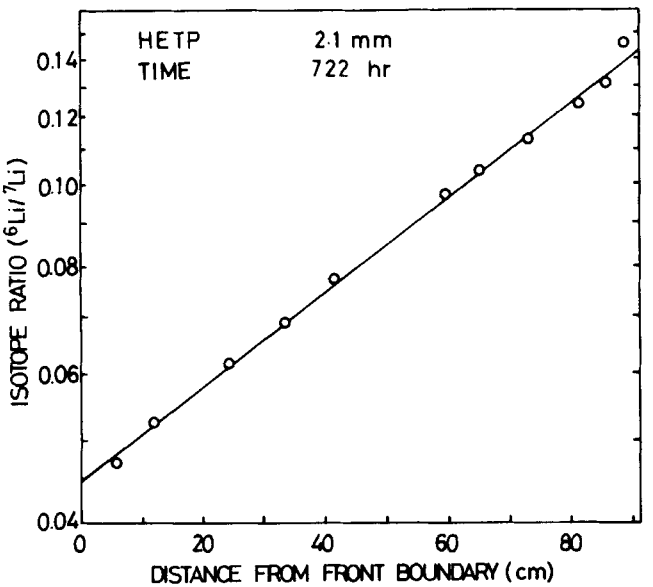

FIG. 9C. The fitting of profiles for the displacement of a 91.1-cm long band.

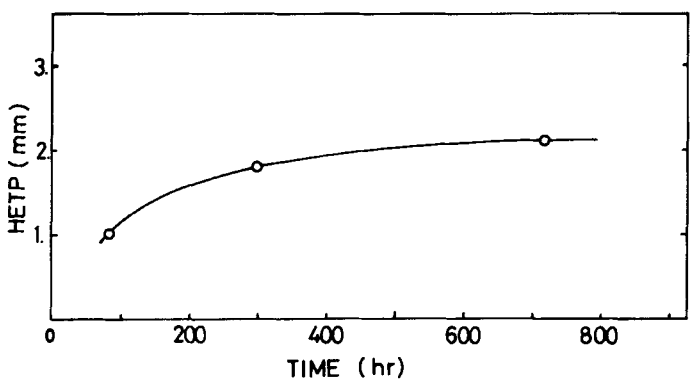

FIG. 10. The values of HETP obtained.

for the displacement of the 7-m and 91.1-cm long bands, corresponds to heights of the liquid volume of about 5.8 and 3.6 cm, respectively. This tendency is consistent with that of the overlapping lengths at the boundaries of lithium bands. We have to operate the circuit while making the liquid volumes above the beds as small as practicable in order to gain a high performance of isotope separation. Furthermore, the possibility of "tilting" and "channeling" the flow might increase with time in the columns. Liquid mixing in various parts of columns affects the concentration profiles. This has been confirmed by experiments (*18, 19*).

As for the displacement distance *Le* (cm) necessary for the attainment of the steady state, Powell presented the approximate equation (*3*)

$$Le = (\text{band length})/(\alpha - 1) \tag{17}$$

which is often used in the literature. However, this is not applicable in the present experiment. The steady state is attained at distances of 128.5 and 41.6 m for the displacement of the 91.1- and 56.3-cm long bands, respectively. Nevertheless, the equation gives distances of 325 and 201 m for the respective cases.

CONCLUSION

Lithium isotope separation is carried out by means of a circuit for continuous displacement chromatography by using sodium acetate as the displacement reagent, and the isotope concentration profiles are obtained at the steady and unsteady states. These profiles agreed well with the theory of continuous countercurrent separation in total reflux operation, assuming appropriate values for HETP. The values of HETP obtained are found to increase gradually during the displacement operation, and they level off at the steady state value. The phenomenon is considered to be due to liquid mixing in the columns.

Acknowledgments

The authors gratefully acknowledge the assistance of T. Itoi (Mitsubishi Chemical Industries Ltd.) in obtaining the data. They also wish to acknowledge the technical suggestions of Drs J. Shimokawa, K. Iwamoto and Y. Naruse of the Japan Atomic Energy Research Institute.

REFERENCES

1. T. I. Taylor and H. C. Urey, *J. Chem. Phys., 6*, 429 (1938).
2. E. Glueckauf, K. H. Baker, and G. P. Kitt, *Faraday Soc. Discuss., 7*, 199 (1949).
3. J. E. Powell, *J. Inorg. Nucl. Chem., 24*, 183 (1962).
4. D. A. Lee and G. M. Begun, *J. Am. Chem. Soc., 81*, 2332 (1959).
5. D. A. Lee, *J. Phys. Chem., 64*, 187 (1960).
6. D. A. Lee, *J. Chem. Eng. Data, 6*(4), 565 (1961).
7. D. A. Lee, *J. Am. Chem. Soc., 83*, 1801 (1961).
8. D. A. Lee and J. S. Drury, *J. Inorg. Nucl. Chem., 27*, 1405 (1965).
9. R. E. Blanco and J. T. Roberts, *J. Nucl. Energy, Part B, 3*, 161 (1962).
10. Z. Hagiwara and Y. Takakura, *J. Nucl. Sci. Technol., 6*(5), 279 (1969).
11. Z. Hagiwara and Y. Takakura, *Ibid., 6*(6), 326 (1969).
12. Z. Hagiwara and Y. Takakura, in *Recent Development in Mass Spectroscopy* (Proc. Int. Conf. Mass Spect., Kyoto, September 1969), University of Tokyo Press., p. 383.
13. S. Fujine, *Sep. Sci. Technol.*, Accepted for Publication.
14. E. Glueckauf, *J. Am. Chem. Soc., 81*, 5262 (1959).
15. S. Fujine, K. Saito, Y. Naruse, K. Shiba, M. Kosuge, T. Itoi, and T. Kitsukawa, *JAERI-M 9735*, 1981 (in Japanese).
16. F. U. Spedding, J. E. Powell, and H. J. Svec, *J. Am. Chem. Soc., 77*, 6125 (1955).
17. T. Nakajima, H. Fukushima, and S. Fujine, *41th Conf. Anal. Chem. Soc. Jpn., 1C11*, 162 (1980) (in Japanese).
18. S. Fujine, K. Saito, K. Iwamoto, and T. Itoi, *JAERI-M 9573*, 1981 (in Japanese).
19. F. Helfferich, in *Ion Exchange*, McGraw-Hill, New York, 1962, p. 486.

Received by editor March 16, 1982